The Selective Ammoximation of Ketones via in-situ H_2O_2 Synthesis.

Richard J. Lewis[a*], Kenji Ueura[b], Xi Liu[c*], Yukimasa Fukuta[b], Tian Qin[c], Thomas E. Davies[a], David J. Morgan[a,d], Alex Stenner[a], James Singleton[a], Jennifer. K. Edwards[e], Simon J. Freakley[f], Christopher J. Kiely[g], Liwei Chen[c,h], Yasushi Yamamoto[b] and Graham J. Hutchings [a*]

[a]Max Planck–Cardiff Centre on the Fundamentals of Heterogeneous Catalysis FUNCAT, Cardiff Catalysis Institute, School of Chemistry, Cardiff University, Main Building, Park Place, Cardiff, CF10 3AT, UK.

[b]UBE Corporation, 1978-5, Kogushi, Ube, Yamaguchi 755-8633, Japan.

[c]School of Chemistry and Chemical, In-situ Centre for Physical Sciences, Shanghai Jiao Tong University, 200240, Shanghai, P. R. China.

[d]HarwellXPS, Research Complex at Harwell (RCaH) Didcot, OX11 0FA, UK

[e]Cardiff Catalysis Institute, School of Chemistry, Cardiff University, Main Building, Park Place, Cardiff, CF10 3AT, UK.

[f]Department of Chemistry, University of Bath, Claverton Down, Bath, BA2 7AY, UK

[g]Department of Materials Science and Engineering, Lehigh University, Bethlehem, PA 18015, USA

[h]School of Chemistry and Chemical, Frontiers Science Centre for Transformative Molecules, Shanghai, 200240, P.R. China

*LewisR27@cardiff.ac.uk, LiuXi@sjtu.edu.cn, Hutch@cardiff.ac.uk

Abstract.

The ammoximation of ketones to the corresponding oxime via the in-situ production of H_2O_2, offers an attractive alternative to the current means of production, particularly that of cyclohexanone oxime, a key precursor to Nylon-6. Herein, we demonstrate that using a bifunctional catalyst, consisting of Pd-based bimetallic nanoparticles immobilised onto a TS-1 carrier, it is possible to bridge the considerable conditions gap that exists between the two distinct reaction pathways (H_2O_2 direct synthesis and ketone ammoximation). The formation of PdAu nanoalloys is found to be crucial in achieving high catalytic performance and stability, with the bimetallic PdAu catalyst significantly outperforming both the monometallic Pd analogue and a range of other Pd-based materials.

Keywords: Green Chemistry, Industrial Catalysis, Feedstock Valorisation, Ketone Ammoximation, Hydrogen Peroxide, Palladium-Gold.

Introduction.

Since first developed by EniChem, (1) the combination of the titanosilicate TS-1 and preformed H_2O_2 has found significant application in the chemical synthesis sector, (2) achieving excellent activities and selectivities for aromatic hydroxylation, (3) the oxidative dehydrogenation of alkanes(4) and alkene epoxidation.(5) The most pertinent examples of major industrial processes that utilise commercial H_2O_2 in conjunction with TS-1 are perhaps the integrated hydrogen peroxide to propylene oxide (HPPO) process(6-7) and the ammoximation of cyclohexanone to cyclohexanone oxime,(8) a key precursor in the production of the polyamide Nylon-6. With global demand for Nylon-6 estimated to exceed 8.9 million tons per annum by 2026,(9) largely driven by its application as an industrial fibre and textile, a concurrent rise in cyclohexanone oxime production is likewise expected.(10)

The conventional approach to cyclohexanone oxime production, which reacts cyclohexanone with hydroxylamine salts is considered to be highly inefficient, producing large quantities of low-value by-products, such as ammonium sulphate.(11-12) However, the development of the EniChem route, which utilises TS-1 with preformed H_2O_2 in conjunction with ammonia, largely overcame these efficiency concerns, achieving selectivities towards the oxime typically in excess of 95%.(13-14) It is widely considered that the H_2O_2/TS-1 route proceeds via an intermediate hydroxylamine species, which is synthesised over the Ti^{IV} sites present within the titanosilicate framework.(15) This subsequently reacts non-catalytically with cyclohexanone to produce the oxime. Despite the high oxime selectivity and efficiency of the industrial ammoximation process the addition of preformed H_2O_2 in stoichiometric excess is typically required,(16) due to the low stability of the oxidant under ammoximation reaction

conditions, namely elevated temperatures and a basic reaction medium, resulting in an associated increase in process costs.

Furthermore, the industrial ammoximation process is hampered by the significant drawbacks associated with the means by which H_2O_2 is produced on an industrial scale, the anthraquinone oxidation process, which accounts for approximately 95 % of global H_2O_2 production.(17) These include low atom efficiency and high infrastructure costs, with the latter often dictating that H_2O_2 production is prohibited at the point of use and necessitating the transport and storage of H_2O_2 at concentrations far in excess of that required by the end user, with the energy utilised in the concentration process effectively wasted when H_2O_2 is diluted to desirable concentrations.(18-19) In addition, the instability of H_2O_2 at relatively mild temperatures requires the use of acidic stabilizing agents, to prevent decomposition to H_2O during transport and storage. Such additives can promote reactor corrosion, limit catalyst lifetime and result in complex product streams, adding further cost to any industrial process that utilised preformed H_2O_2.(20) Likewise all systems that utilise commercial H_2O_2 can be considered to suffer from these same inefficiencies to a certain extent.

The decoupling of oxidative transformations, such as cyclohexanone ammoximation, from off-site H_2O_2 production, would potentially lead to considerable economic savings, and a reduction in greenhouse gas emissions, representing a positive step toward more sustainable industrial processes. To this end, several studies have investigated the efficacy of alternative approaches that would avoid large-scale H_2O_2 production and allow for the on-site production and direct utilisation of H_2O_2. However, to date, these systems have not been simple or robust enough for adoption on an industrial scale. For example, the supply of H_2O_2 via the partial oxidation of isopropanol as described by Liang *et al*. (21) and Zajacek *et al.* (22) yields appreciable concentrations of impurities, producing an undesirable and complex product mixture. By comparison, the in-situ production of H_2O_2 from molecular H_2 and O_2 would negate the significant drawbacks associated with commercially synthesised H_2O_2, while avoiding the dilution of product streams through the continual addition of an aqueous oxidant and could offer an overall reduction in process costs.

A proposed reaction for the ammoximation of cyclohexanone via in-situ H_2O_2 synthesis is outlined in Scheme 1 and can be considered to be comparable to the current industrial process where the preformed oxidant is continually supplied.(1) In the case of the in-situ approach, immobilised precious metal species are responsible for the formation of the oxidant, which is subsequently utilised in the formation of hydroxylamine by Ti^{IV} sites present within the TS-1 framework, with the intermediate species subsequently reacting non-catalytically with the ketone to synthesise the corresponding oxime in the liquid phase. In order to achieve maximal

process efficiency, there is clearly a need to balance the rate of H_2O_2 synthesis over the metal component with that of hydroxylamine formation and inhibit competitive H_2O_2 degradation reactions catalysed by metal species, which limit selective utilisation of H_2.

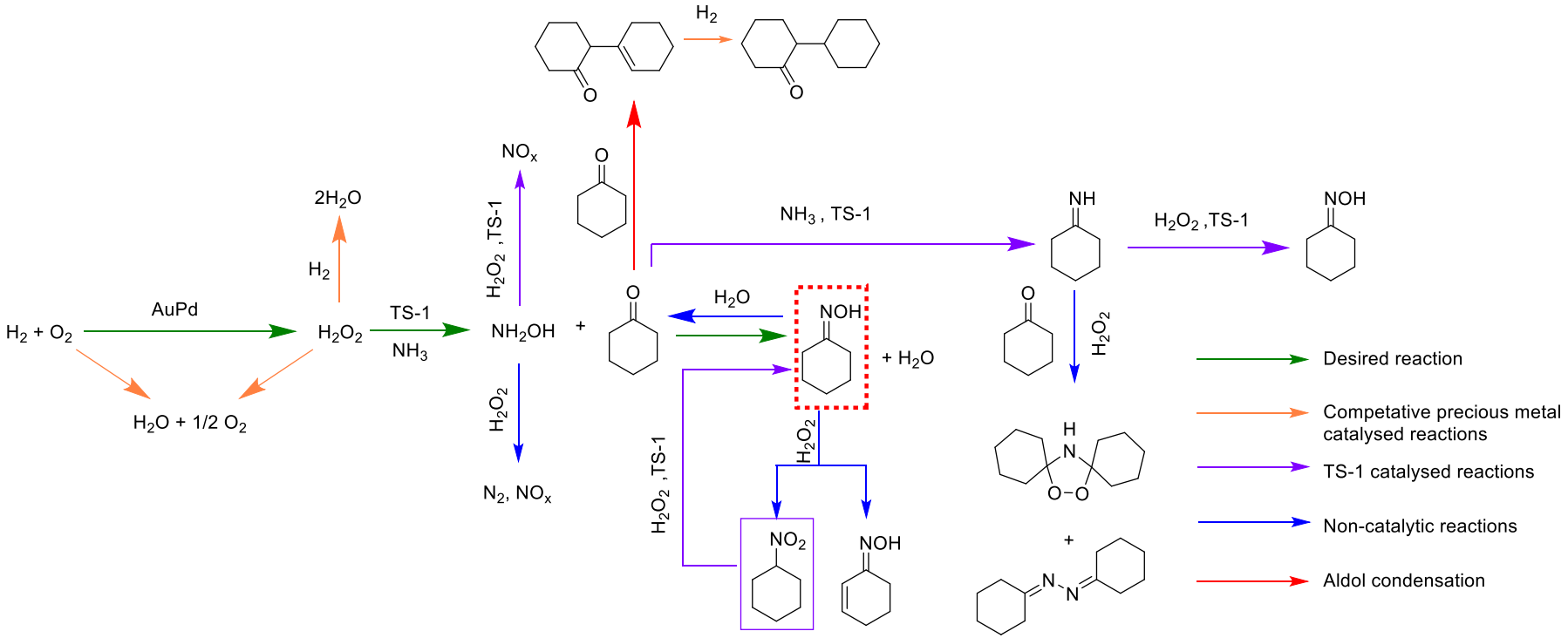

Scheme 1. Proposed reaction scheme for the ammoximation of cyclohexanone to the corresponding oxime, via in-situ H_2O_2 synthesis.

We have recently demonstrated that it is possible to achieve high selectivities towards cyclohexanone oxime production via the in-situ synthesis of H_2O_2, (23) overcoming the considerable conditions gap that exists between these two critical processes, with the direct synthesis of H_2O_2 favoured by acidic conditions(24-26) and sub-ambient temperatures(27) while cyclohexanone ammoximation is associated with elevated temperatures (80-140 °C) and utilises ammonia. Building on this previous study, which focussed extensively on a tandem system, consisting of a H_2O_2 synthesising catalyst used in conjunction with a commercially available TS-1, we now focus on a composite bifunctional catalyst, that is able to both synthesise H_2O_2 and subsequently utilise the oxidant in the production of cyclohexanone oxime.

Experimental.

Catalyst Preparation.

Mono- and bi-metallic 0.66%Pd-X/TS-1 (where Pd: X = 1:1 (wt / wt) and X = Au, Pt, Ni, Cu, Rh, Ir, Co, Mn, Ga, Ag, Sn, Ru, In) catalysts have been prepared by a wet co-impregnation procedure, based on a methodology previously reported in the literature. (28) The procedure to produce the 0.33%Pd-0.33%Au/TS-1 catalyst (2 g) is outlined below with a similar methodology utilised for all mono- and bi-metallic analogues. The requisite amounts of metal precursor used for the synthesis of key catalysts is reported in Table S.1.

$PdCl_2$ (1.100 mL, [Pd] = 6.00 $mgmL^{-1}$, Sigma Aldrich) and $HAuCl_4.3H_2O$ (0.539 mL, [Au] = 12.25 $mgmL^{-1}$, Strem Chemicals) were charged into a 50 mL round bottom flask, with total volume adjusted to 16 mL using H_2O (HPLC grade, Fischer Scientific). The resulting mixture was heated to 65 °C in a thermostatically controlled oil bath with stirring (600 rpm). Upon reaching the requisite temperature TS-1 (1.987 g, HighChem), was added over the course of 5 minutes. The resulting slurry was then heated to 85 °C for 16 h to allow for complete evaporation of water. The resulting solid material was ground prior to calcination in static air (typically 400 °C, 3 h, 10 °C min^{-1}).

Catalyst Testing.

Note 1: Reaction conditions used within this study operate below the flammability limits of gaseous mixtures of H_2 and O_2.

Note 2: The conditions used within this work for H_2O_2 synthesis and degradation have previously been investigated, with the use of sub-ambient reaction temperatures, CO_2 reactant gas diluent and a methanol co-solvent identified as key to maintaining high catalytic efficacy towards H_2O_2 production. (27)

Note 3: In all cases, reactions were run multiple times, over multiple batches of catalyst, with the data presented an average of these experiments.

Direct synthesis of H_2O_2.

Hydrogen peroxide synthesis was evaluated using a Parr Instruments stainless steel autoclave with a nominal volume of 100 mL, equipped with a PTFE liner and a maximum working pressure of 2000 psi. To test each catalyst for H_2O_2 synthesis, the autoclave was charged with catalyst (0.01 g) and solvent (5.6 g MeOH and 2.9 g H_2O, both HPLC grade, Fischer Scientific). The charged autoclave was then purged three times with 5%H_2/CO_2 (100 psi) before filling with 5% H_2 / CO_2 (420 psi), followed by the addition of 25%O_2/CO_2 (160 psi) to give a H_2: O_2 ratio of 1: 2. All pressures are provided as gauge pressures, reactant gases were not continuously introduced into the reactor. The temperature was then decreased to 2 °C (using a HAAKE K50 bath/circulator and an appropriate coolant) followed by stirring (1200 rpm) of the reaction mixture for 0.5 h. H_2O_2 productivity was determined by titrating aliquots of the final solution after reaction with acidified $Ce(SO_4)_2$ (0.01 M) in the presence of ferroin indicator.

Degradation of H_2O_2.

Catalytic activity towards H_2O_2 degradation (via hydrogenation and decomposition pathways) was determined in a manner similar to that used for measuring the H_2O_2 direct synthesis activity of a catalyst. The autoclave was charged with methanol (5.6 g, HPLC grade, Fisher Scientific), H_2O_2 (50 wt.% 0.69 g, Merck), H_2O (2.21 g, HPLC grade, Fisher Scientific) and catalyst (0.01 g), with the solvent composition equivalent to a 4 wt.% H_2O_2 solution. From the solution, two aliquots of 0.05 g were removed and titrated with acidified $Ce(SO_4)_2$ solution using ferroin as an indicator to determine an accurate concentration of H_2O_2 at the start of the reaction. The charged autoclave was then purged three times with 5%H_2/CO_2 (100 psi) before filling with 5%H_2/CO_2 (420 psi). All pressures are provided as gauge pressures, reactant gases were not continuously introduced into the reactor. The reaction mixture was cooled to 2 °C prior to the reaction commencing upon stirring (1200 rpm). The reaction was allowed to proceed for 0.5 h, after which, the catalyst was removed from the reaction solvents via filtration and as described previously, two aliquots of 0.05 g were titrated against the acidified $Ce(SO_4)_2$ solution using ferroin as an indicator. Catalyst degradation activity is reported as $mol_{H2O2}kg_{cat}^{-1}h^{-1}$.

Ketone ammoximation via the in-situ synthesis of H_2O_2.

Catalysts were evaluated for their activity towards ketone ammoximation with the procedure for cyclohexanone ammoximation outlined below using a stainless-steel autoclave (Parr Instruments) with a nominal volume of 100 mL, equipped with a PTFE liner and a maximum working pressure of 2000 psi.

The autoclave was charged with the catalyst (0.075 g), solvent (H_2O (7.5 g, HPLC grade, Fisher Scientific) and t-BuOH (5.9 g, Merck)), cyclohexanone (0.196 g, 2.0 mmol, Merck) and ammonium bicarbonate (0.32 g, 4.0 mmol, Merck). With t-BuOH chosen as co-solvent due to the enhanced solubility of H_2, in comparison to H_2O, and the ability of t-BuOH to aid in the maintenance of the -Ti-O-Si- moiety, known to be responsible for the high activity of TS-1. (29) The reactor was purged three times with 5%H_2/N_2 (100 psi) and then filled with 5%H_2/N_2 (420 psi) and 25%O_2/N_2 (160 psi) to give a H_2: O_2 ratio of 1: 2. All pressures are provided as gauge pressures, reactant gases were not continuously introduced into the reactor. The reactor was stirred (100 rpm) while the reaction temperature was raised to 80 ^{O}C at which time stirring was increased to 800 rpm. The reaction was allowed to run for 6 h, unless otherwise stated, after which the reactor was cooled to 25 °C while stirring (100 rpm), using ice water. The reactant gas was collected for analysis gas chromatography using a Varian CP-3380 equipped with a TCD and a Porapak Q column. To the reaction solution, EtOH (6 g, HPLC grade, Fischer Scientific) and diethylene glycol monoethyl ether (external standard, 0.15 g, Merck) were added, with the former used to ensure complete homogeneity of the post-reaction solution, while the latter was chosen as an external standard. Following this, the catalyst was removed by filtration and the resulting solution was analysed by gas chromatography using a Varian 3800 equipped with FID and a CP-Wax 52 CB column.

For reactions conducted in the presence of H_2 or O_2 alone, the pressure of the reagent (5%H_2/N_2 or 25%O_2/N_2) was identical to that used in the in-situ reaction, with total pressure maintained at 580 psi using N_2. For reactions using commercial H_2O_2 (50 wt.%, Fischer Scientific) the concentration of H_2O_2 utilised was identical to that which may be generated if all the H_2 in the in-situ reaction was converted to H_2O_2, in this case, the oxidant was added to the reaction mixture, prior to the reaction starting and replaced part of the H_2O component, again total pressure was maintained using N_2 (580 psi).

For reactions utilizing ketones other than cyclohexanone (cyclopentanone, cycloheptanone, cyclooctenone and cyclododecanone) all chemicals were purchased from Merck. For calibration purposes, cyclohexanone oxime and cyclododecanone oxime were purchased from Merck. Cyclopentanone oxime and cycloctanone oxime were purchased from Alfa Aesar, while cycloheptanone oxime was purchased from ChemCruz. All chemicals were used as received.

Ketone conversion and selectivity towards the oxime were calculated on the basis of starting amount of the ketone, according to Eqs. (1) and (2), respectively.

$$X_{ketone} = \frac{n_{ketone\,(t(0))} - n_{ketone\,(t(1))}}{n_{ketone\,(t(0))}}\ x\ 100 \quad (1)$$

$$S_{oxime} = \frac{n_{oxime}}{n_{ketone\,(t(0))} - n_{ketone\,(t(1))}}\ x\ 100 \quad (2)$$

Total autoclave capacity was determined via water displacement to allow for accurate determination of H_2 conversion and oxime selectivity based on H_2. When equipped with a PTFE liner (reducing nominal volume to 66 mL) the total volume of an unfilled autoclave was determined to be 93 mL, which includes all available gaseous space within the autoclave.

H_2 conversion and selectivity based on H_2 were calculated on the basis of starting amount of H_2 and the yield of oxime as determined from Eqs. (3) and (4).

$$X_{H2} = \frac{n_{H2\,(t(0))} - n_{H2\,(t(1))}}{n_{H2\,(t(0))}}\ x\ 100 \quad (3)$$

$$S_{H2} = \frac{n_{oxime}}{\left(\frac{n_{H2\,(t(0))} - n_{H2\,(t(1))}}{n_{H2\,(t(0))}}\right)}\ x\ 100 \quad (4)$$

Time-on-line analysis for ketone ammoximation via the in-situ synthesis of H_2O_2.

An identical procedure to that outlined above for ketone ammoximation via the in-situ production of H_2O_2 is followed for the desired reaction time. It should be noted that individual experiments were carried out and the reaction mixture was not sampled on-line.

Hot filtration experiments for ketone ammoximation via the in-situ synthesis of H_2O_2.

Catalytic activity is determined in a similar manner to that outlined above for ketone ammoximation using a 0.66%PdAu/TS-1 catalyst (0.075 g). After a 1.5 h reaction the solid catalyst was removed by filtration from the reaction solution and replaced with bare TS-1 (0.075 g, HighChem), with the reaction solution returned to the autoclave. The reactor was

then re-charged with reagent gases (5%H_2/N_2 (420 psi) and 25%O_2/N_2 (160 psi) and allowed to proceed for a further 1.5 h as described above. In this case the bare TS-1 was used as received.

Catalyst reusability in the ammoximation of ketones via the in-situ synthesis of H_2O_2.

In order to determine catalyst reusability, a similar procedure to that outlined above for ketone ammoximation via the in situ production of H_2O_2 was followed utilizing 0.3 g of catalyst. Following the initial test, the catalyst was recovered by filtration, washed with EtOH (6 g, Fischer Scientific) and dried (30 °C, 17 h, under vacuum). Next, 0.075 g of material from the recovered catalyst sample was used to conduct a standard ammoximation experiment.

Catalyst characterisation.

Investigation of the bulk structure of the crystalline materials was carried out using a (θ-θ) PANalytical X'pert Pro powder diffractometer using a Cu K_α radiation source, operating at 40 KeV and 40mA. Standard analysis was carried out using a 40 min run with a back filled sample, between 2θ values of 10 – 80°. Phase identification was carried out using the International Centre for Diffraction Data (ICDD).

Note 4: X-ray diffractograms of key as-prepared catalysts are reported in Figure S.1, with no reflections associated with active metals, indicative of the relatively low total loading of the immobilised metals.

X-ray photoelectron spectroscopy (XPS) analyses were made on a Kratos Axis Ultra DLD spectrometer. Samples were mounted using double-sided adhesive tape and binding energies were referenced to the C(1s) binding energy of adventitious carbon contamination taken to be 284.8 eV. Monochromatic AlK_α radiation was used for all measurements; an analyser pass energy of 160 eV was used for survey scans while 40 eV was employed for detailed regional scans. The intensities of the Au(4f) and Pd(3d) features were used to derive the Au / Pd surface ratios and Ti(2p) and Si(2p) features used to derive the Si / Ti surface ratios. All data was processed using CasaXPS v2.3.24 using a Shirley background, and modified Wagner elemental sensitivity factors as supplied by the instrument manufacturer.

Note 5: Given the low metal loading of these materials and the propensity for analysis-induced reduction the XP data were acquired in an optimised time frame to minimise such reduction but still with a workable signal-to-noise ratio.

Fourier-transform infrared spectroscopy (FTIR) was carried out with a Bruker Tensor 27 spectrometer fitted with a HgCdTe (MCT) detector and operated with OPUS software.

Diffuse reflectance infrared Fourier transform spectroscopy (DRIFTS) measurements were taken on a Bruker Tensor 27 spectrometer fitted with a mercury cadmium telluride (MCT)

detector. A sample was loaded into the Praying Mantis high temperature (HVC-DRP-4) in-situ cell before exposure to N_2 and then 1% CO/N_2 at a flow rate of 50 $cm^3\,min^{-1}$. A background spectrum was obtained using KBr, and measurements were recorded every 1 min at room temperature. Once the CO adsorption bands in the DRIFT spectra ceased to increase in size, the gas feed was changed back to N_2 and measurements were repeated until no change in subsequent spectra was observed.

Metal leaching was quantified via analysis of post-reaction solutions via inductively coupled plasma mass spectrometry (ICP-MS) using an Agilent 7900 ICP-MS equipped with an I-AS auto-sampler using a 5-point calibration using certified reference materials from Perkin Elmer and certified internal standard from Agilent. All calibrants were matrix matched.

Transmission electron microscopy (TEM) was performed on a JEOL JEM-2100 operating at 200 kV. Samples were prepared by dry deposition onto 300 mesh copper grids coated with holey carbon film.

Aberration corrected scanning transmission electron microscopy (AC-STEM) was performed using a probe-corrected Hitachi HF5000 S/TEM, operating at 200 kV. The instrument was equipped with bright field (BF) and high angle annular dark field (HAADF) detectors for high spatial resolution STEM imaging experiments. This microscope was also equipped with a secondary electron detector and dual Oxford Instruments XEDS detectors (2 x 100 mm^2) having a total collection angle of 2.02 sr. Additional aberration corrected scanning transmission electron microscopy was performed using a ThermoFisher ThemisZ S/TEM, operating at 300 keV. The instrument was equipped with high angle annular dark field (HAADF) and a segmented DF4 detector for high spatial resolution for high spatial resolution STEM-HAADF and STEM-iDPC imaging experiments. The installed Super-X detector has a total area of 120 mm^2 and 0.7 sr solid angle. In-situ measurements were also conducted using the Hitachi HF5000 instrument. The catalytic materials were heated from ambient temperature to 400 °C and analysed by STEM-ADF and XEDS to identify structural and compositional changes during oxidative heat treatment.

Results and Discussion.

Our initial investigations established the efficacy of a range of Pd-based, TS-1 supported, bimetallic catalysts, prepared by a wet co-impregnation procedure, towards the direct synthesis and subsequent degradation of H_2O_2 (Table S.2). These experiments were carried out under reaction conditions previously optimised to enhance H_2O_2 stability, namely the presence of sub-ambient temperatures, a methanol co-solvent and a CO_2 gaseous diluent, all of which contribute to the inhibition of H_2O_2 degradation pathways.(27) The limited activity of the bimetallic catalysts towards H_2O_2 production was clear, with the exception of the 0.33%Pd-0.33%Pt/TS-1 (38 $mol_{H2O2}kg_{cat}^{-1}h^{-1}$) and 0.33%Pd-0.33%Au/TS-1 (44 $mol_{H2O2}kg_{cat}^{-1}h^{-1}$) formulations. Perhaps unexpectedly, given the extensive literature reporting the improved

catalytic performance that can be achieved from the alloying of Pd with Au(30-32) the H_2O_2 synthesis activity of the 0.66%Pd/TS-1 catalyst (66 $mol_{H2O2}kg_{cat}^{-1}h^{-1}$) was found to be superior to the PdAu analogue, which may suggest a lack of the synergistic enhancement often reported for bimetallic PdAu catalysts. (33,34) However, it is important to note that the rate of H_2O_2 synthesis over the 0.33%Pd-0.33%Au/TS-1 catalyst was far greater than that of the 0.33%Pd/TS-1 analogue (28 $mol_{H2O2}kg_{cat}^{-1}h^{-1}$). When also considering the limited activity of the 0.33%Au/TS-1 catalyst (2 $mol_{H2O2}kg_{cat}^{-1}h^{-1}$), it is possible to conclude that the observed activity of the bimetallic formulation is not cumulative and a synergistic enhancement does indeed result from the alloying of the two metals. Although it may be possible to consider such an improvement exists to a lesser extent than that previously reported for a range of supported PdAu catalysts. (35,36)

In keeping with the poor performance of the majority of the bimetallic catalysts towards H_2O_2 production, activity towards the ammoximation of cyclohexanone via the in-situ production of H_2O_2 was also found to be limited, again with the exception of the 0.33%Pd-0.33%Pt/TS-1 (69% oxime yield) and 0.33%Pd-0.33%Au/TS-1 (95% oxime yield) catalysts (Figure 1). The significant improvement in cyclohexanone ammoximation activity in the presence of H_2 and O_2 compared to that observed when using either reagent alone should also be noted (Figure S.2). Indeed, the in-situ approach also offers increased cyclohexanone oxime yields compared to that observed when using preformed H_2O_2 (70% oxime yield), at a concentration of H_2O_2 comparable to that present if all the H_2 in the in-situ reaction was converted to H_2O_2. The relatively limited activity observed when using commercial H_2O_2 can be attributed to the complete addition of H_2O_2 at the start of the reaction, with the continual incremental addition of H_2O_2 over the course of the ammoximation reaction well known to influence the catalytic performance of the current industrial process.(37)

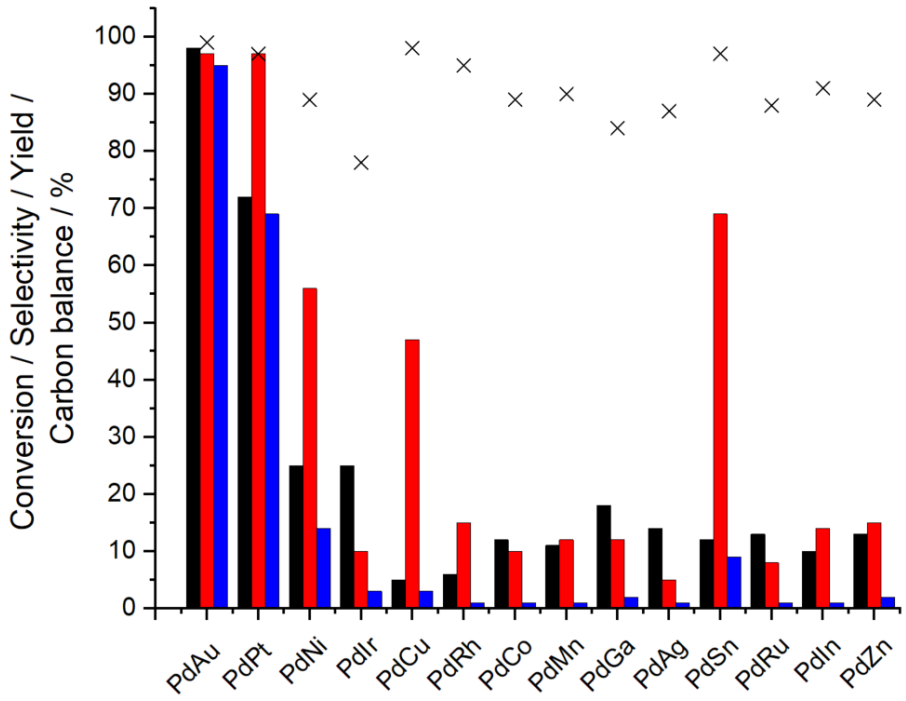

Figure 1. Catalytic activity of TS-1 supported Pd-based catalysts towards the ammoximation of cyclohexanone via the in-situ synthesis of H_2O_2. **Ammoximation reaction conditions:** Ketone (2 mmol), NH_4HCO_3 (4 mmol), 5%H_2/N_2 (4.7 mmol), 25%O_2/N_2 (6.1 mmol), catalyst (0.075 g), t-BuOH (5.9 g), H_2O (7.5 g), 6 h, 80 ^{O}C 800 rpm. ***Key*****;** Cyclohexanone conversion *(black bars*), oxime selectivity (*red bars*), oxime yield (*blue bars*) and carbon balance (*crosses*). **Note 1:** Total metal loading is 0.66 wt.% with Pd: X ratio = 1: 1 (wt/wt). **Note 2:** All catalysts were exposed to an oxidative heat treatment prior to testing (static air, 400 °C, 3 h, 10 °Cmin^{-1}).

The synergy resulting from the alloying of Pd and Au has been extensively studied for the direct synthesis of H_2O_2(30, 38-40) and a range of selective oxidative transformations (using O_2 (41-42) and H_2O_2 (43-44)), with similar observations made within this work for H_2O_2 direct synthesis (Table S.2). Likewise the activity of the bimetallic 0.33%Pd-0.33%Au/TS-1 catalyst towards cyclohexanone ammoximation was also found to greatly exceed that observed over the 0.66%Au/TS-1 (2% oxime yield) or 0.66%Pd/TS-1 (10% oxime yield) analogues (Figure 2), with the enhanced activity of the bimetallic formulation further highlighted through comparison of catalytic performance as a function of reaction time (Table S.3) and determination of apparent reaction rate (Table S.4). Importantly we further observed that when the in-situ ammoximation reaction was not limited by cyclohexanone availability (20% cyclohexanone conversion at 1.5 h over the 0.33%Pd-0.33%Au/TS-1 catalyst), relatively high selective utilisation of H_2 (*i.e.*, mols of H_2 consumed that lead to the formation of the oxime) could be achieved (84% H_2 selectivity). This metric was found to decrease as the reaction proceeds and the availability of cyclohexanone becomes limited (Table S.3) and can be considered to be associated with the increased non-selective consumption of H_2 through H_2O_2 degradation pathways.

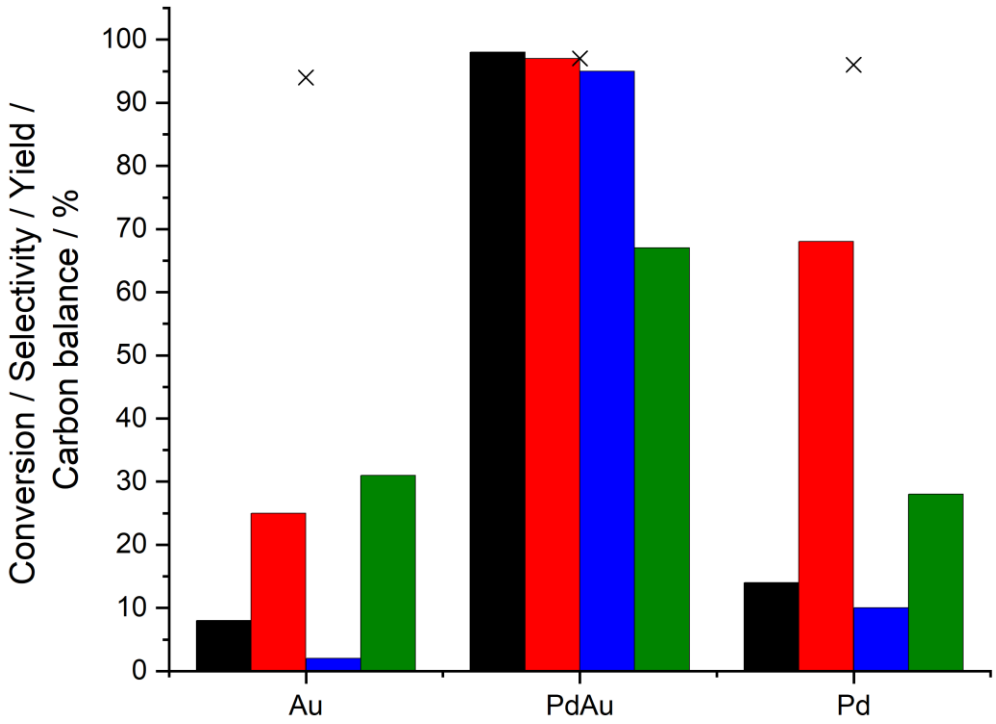

Figure 2. The effect of alloying Au and Pd on catalytic activity towards the ammoximation of cyclohexanone via *in-situ* H_2O_2 production. ***Key*****;** Cyclohexanone conversion *(black bars*), oxime selectivity (*red bars*), oxime yield (*blue bars*), H_2 selectivity (*green bars*) and carbon balance (*crosses*). **Ammoximation reaction conditions:** Cyclohexanone (2 mmol), NH_4HCO_3 (4 mmol), 5%H_2/N_2 (420 psi), 25%O_2/N_2 (160 psi), catalyst (0.075 g), t-BuOH (5.9 g), H_2O (7.5 g), 6 h, 80 °C, 800 rpm. **Note:** Au refers to 0.66%Au/TS-1, Pd to 0.66%Pd/TS-1and PdAu to 0.33%Pd-0.33%Au/TS-1.

The synergistic enhancement observed through the formation of PdAu alloys has been typically attributed to a combination of the disruption of contiguous Pd ensembles and electronic modification, with Au acting as a promoter for Pd. (45-47) Indeed, numerous studies have demonstrated that the introduction of Au into Pd surfaces not only inhibits the cleavage of O-O bonds (in $*O_2$, *OOH or $*H_2O_2$ species), and the resulting formation of H_2O, but also promotes the release of surface-bound H_2O_2. (38,48) These earlier works coupled with the enhanced performance and selectivity of the 0.33%Pd-0.33%Au/TS-1 catalyst suggests that the presence of Au is likely key in facilitating the desorption of H_2O_2 from PdAu surfaces, which subsequently diffuses to Ti^{IV} sites present within the TS-1 framework, where it is utilised in hydroxylamine formation. With the crucial role of Au established, we next investigated the effect of Pd: Au ratio on catalytic performance, while maintaining total metal loading at 0.66 wt.%. In keeping with our previous studies into PdAu nanoparticles supported on TS-1(28) and SiO_2(49) as well as our investigations within this work (Table S.2), catalytic activity towards both the direct synthesis and subsequent degradation of H_2O_2 was found to correlate well with total Pd content. Indeed, the 0.66%Pd/TS-1 catalyst offered a greater activity towards

both the direct synthesis of H_2O_2 (66 $mol_{H2O2}kg_{cat}^{-1}h^{-1}$), as well as its subsequent degradation (209 $mol_{H2O2}kg_{cat}^{-1}h^{-1}$), in comparison to the Au-only or bimetallic analogues (Table S.5).

Evaluation of the performance of the TS-1 supported catalysts towards cyclohexanone ammoximation identified an optimal nominal composition of 0.33%Pd-0.33%Au/TS-1, with this catalyst greatly outperforming either Au-rich or Pd-rich compositions (Figure 3, comparison of apparent rates of reaction shown in Table S.6), with the enhanced activity of all PdAu catalysts compared to monometallic analogues, further highlighting the role of alloy formation in achieving enhanced catalytic performance. The relationship between catalytic activity towards the direct synthesis (and degradation) of H_2O_2 and the in-situ ammoximation of cyclohexanone was subsequently compared (Figure S.3) with such observations highlighting the need for future catalyst development to focus both on catalytic reactivity towards H_2O_2 production and minimising competitive H_2O_2 degradation pathways.

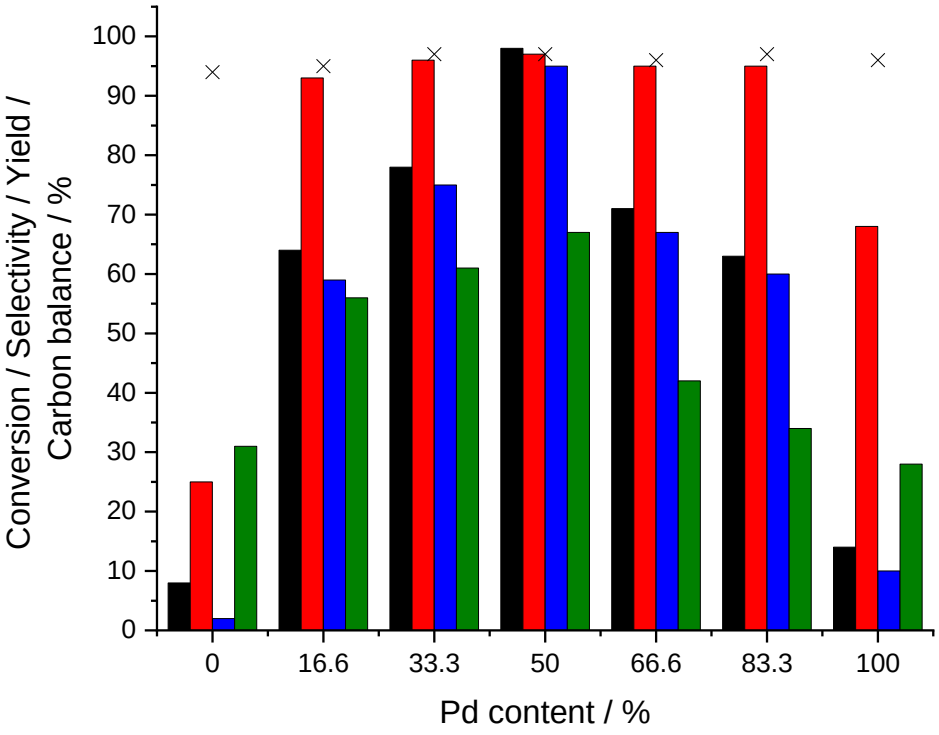

Figure 3. The effect of Pd: Au ratio on the catalytic activity of 0.66%PdAu/TS-1 catalysts towards the ammoximation of cyclohexanone via the *in-situ* production of H_2O_2. ***Key*;** Cyclohexanone conversion *(black bars*), oxime selectivity (*red bars*), oxime yield (*blue bars*), H_2 selectivity (*green bars*) and carbon balance (*crosses*). **Ammoximation reaction conditions:** Cyclohexanone (2 mmol), NH_4HCO_3 (4 mmol), 5%H_2/N_2 (420 psi), 25%O_2/N_2 (160 psi), catalyst (0.075 g), t-BuOH (5.9 g), H_2O (7.5 g), 6 h, 80 °C, 800 rpm.

The catalytic performance of Pd-based catalysts towards H_2O_2 is known to be highly dependent on Pd oxidation state, with a range of studies demonstrating the enhanced efficacy of Pd^{2+}-Pd^0 domains towards H_2O_2 production in comparison to Pd^{2+} or Pd^0 counterparts. (46,50) An analysis of the supported PdAu catalysts via XPS indicates an increase in Pd^0 content with the introduction of Au (Figure S.4). Such observations suggest that, at least in

part, the modification of Pd speciation through alloying with Au may be key to achieving high catalytic efficacy. However, it should be noted that such analysis is not representative of metal speciation in-situ.

With our analysis by XPS demonstrating that the formation of PdAu alloys results in a considerable modification in Pd speciation (Figure S.4) we were subsequently motivated to probe this catalytic series via CO-DRIFTS (Figure S.5). The DRIFTS spectra of all catalysts were found to be dominated by Pd-CO bands, with the exception of the Au-rich formulations (0.66%Au/TS-1 and 0.11%Pd-0.55%Au/TS-1), where a combination of low (or no) Pd content and the transient nature of the Au-CO interaction at ambient temperature is considered the cause for the lack of an observable signal for these formulations. (30) It is possible to attribute the peaks within the higher wavenumber region of the spectra (approx. 2200-2000 cm^{-1}) to CO linearly adsorbed to low coordination Pd sites (i*.e.,* edges or corners), while those centred at lower wavenumbers (2000-1800 cm^{-1}) can be assigned to the multi-fold adsorption of CO on extended Pd domains (*i.e*., species adsorbed in a bidentate or tridentate manner). The alloying of Pd with Au was found to result in a blueshift in the bands related to these bridging CO species. Such a shift is in keeping with observations made by Wilson *et al*. (51) and can be attributed to the formation of PdAu alloys and the resulting charge transfer between Au Pd.(52) As such, based on our combined XPS and CO-DRIFTS analysis it is possible to determine that the observed enhanced activity of the PdAu/TS-1 catalyst, in part, can be related to the electronic modification of Pd through the formation of alloy structures.

With a focus on the optimal 0.33%Pd-0.33%Au/TS-1 formulation, we subsequently broadened our investigation to determine the effect of calcination temperature on catalytic performance. Analysis by Fourier-transform infrared spectroscopy (FTIR) (Figure S.6, Supplementary Note 1) reveals no discernible change in the observed positions of absorption bands compared to the unmodified support material, over the temperature range studied (85-400 °C) suggesting the structure of TS-1 remains unchanged during immobilisation of precious metals and subsequent calcination, which is in keeping with the known high thermal stability of TS-1.(53) Further analysis by XRD (Figure S.7, Supplementary Note 2) corroborates these observations. Notably, no reflections associated with precious metals were observed, which may be expected given the low total metal loading of these materials.

A strong correlation between calcination temperature and catalytic activity toward H_2O_2 synthesis, under conditions optimised for H_2O_2 production, was observed (Table S.7), with the need to expose the catalyst to a minimum temperature of 400 °C (3 h, static air) to ensure stability under H_2O_2 direct synthesis conditions (Table S.8). Despite displaying the greatest activity towards H_2O_2 synthesis (80 $mol_{H2O2}kgcat^{-1}h^{-1}$), the performance of the dried-only catalyst (85 °C, 16 h, static air) towards the in-situ ammoximation of cyclohexanone was found to be extremely limited (6 % oxime yield) (Figure 4). However, upon exposure to an elevated oxidative treatment, cyclohexanone oxime yield increased considerably (95 % oxime yield

after exposure to calcination at 400 °C). Notably, a significant improvement in selective H_2 utilisation was also found to coincide with exposure to increasing calcination temperature. XPS analysis of this subset of materials (Figure S.8, Supplementary Note 3) indicated a stark shift in Pd: Au ratio and the formation of PdO as a result of high-temperature calcination, which may be indicative of nanoparticle agglomeration and Pd surface migration during calcination. (54)

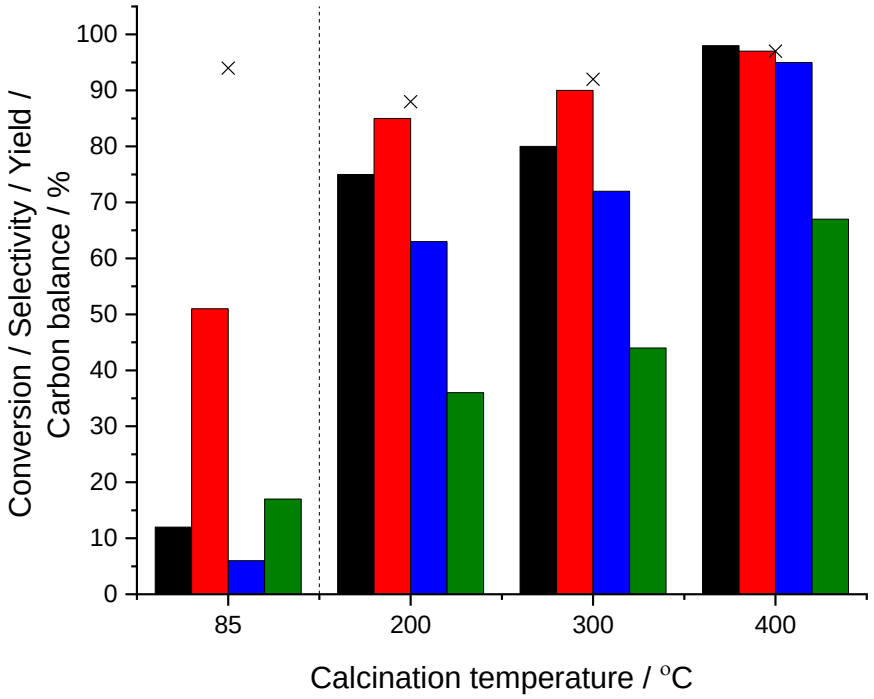

Figure 4. The effect of calcination temperature on catalytic performance of 0.33%Pd-0.33%Au/TS-1 catalyst towards the ammoximation of cyclohexanone via the *in-situ* production of H_2O_2. ***Key*;** Cyclohexanone conversion *(black bars*), oxime selectivity (*red bars*), oxime yield (*blue bars*), H_2 selectivity (*green bars*) and carbon balance (*crosses*). **Ammoximation reaction conditions:** Cyclohexanone (2 mmol), NH_4HCO_3 (4 mmol), 5%H_2/N_2 (420 psi), 25%O_2/N_2 (160 psi), catalyst (0.075 g), t-BuOH (5.9 g), H_2O (7.5 g), 6 h, 80 °C, 800 rpm.

Determination of catalyst stability through ICP-MS analysis of post-reaction solutions revealed considerable leaching of Pd after use in the cyclohexanone ammoximation reaction (Table S.9), particularly for the dried-only catalyst, with this metric found to decrease substantially upon exposure to high-temperature calcination. The leaching of Au was considerably less and decreased to zero with exposure to calcination temperatures of greater than 300 °C. Such observations are in keeping with earlier investigations into supported PdAu catalysts for a range of chemical transformations,(55) including the direct synthesis of H_2O_2,(56) with the improved stability that results from high-temperature oxidative treatment attributed to enhanced metal-support interactions.(36, 57) It should be noted that we have recently demonstrated the improved stability of PdAu alloys, when compared to Pd-only species,

during the in-situ ammoximation of cyclohexanone, and identified that it is the ammonia reagent which is primarily responsible for the observed leaching of Pd.(23) As such it is possible that the observed decrease in Pd leaching as a result of oxidative thermal treatment is indicative of the formation of bimetallic alloys.

TEM analysis of the 0.33%Pd-0.33%Au/TS-1 catalyst indicated the limited immobilisation of the active metal species onto the majority TS-1 component (Figure S.9), with further HAADF-STEM analysis highlighting the preferential deposition onto the minority TiO_2 component (Figure S.10). A degree of variation in mean particle size was observed, regardless of the calcination temperature employed (Table 1). However, based on TEM analysis a major proportion of metal nanoparticles in all samples were found to be below 10 nm, with a number of very large particles (>20 nm) also detected, which is typical of the wet impregnation route to catalyst preparation. (58,59) Our TEM analysis also revealed a shift in mean nanoparticle size upon calcination at elevated temperatures, with this metric increasing from 3.8 nm for the dried-only material to 6.6 nm for the analogous catalyst exposed to a calcination temperature of 400 °C, although it is again worth highlighting that a significant proportion of the smaller (<10 nm) immobilised species are retained despite exposure to high-temperature calcination.

Table 1. Effect of calcination temperature on the mean particle size of the 0.33%Pd-0.33%Au/TS-1 catalyst, as determined by TEM.

Calcination temperature / °C	Mean particle size/nm (S.D)	Productivity / $mol_{H2O2}kg_{cat}^{-1}h^{-1}$[a]	Oxime Yield / %[b]
Dried Only	3.8 (2.5)	80	6
200	3.8 (3.9)	62	63
300	6.2 (5.6)	53	72
400	6.6 (9.1)	44	95

[a]**H_2O_2 direct synthesis reaction conditions:** Catalyst (0.01g), H_2O (2.9g), MeOH (5.6g), 5% H_2 / CO_2 (420 psi), 25% O_2 / CO_2 (160 psi), 0.5 h, 2 ^{O}C 1200 rpm. [b]**Ammoximation reaction conditions:** Cyclohexanone (2 mmol), NH_4HCO_3 (4 mmol), 5%H_2/N_2 (4.7 mmol), 25%O_2/N_2 (6.1 mmol), catalyst (0.075 g), t-BuOH (5.9 g), H_2O (7.5 g), 6 h, 80 ^{O}C, 800 rpm. **Note:** The dried-only catalyst was treated at 85 °C, 16 h, static air.

Analysis of the dried-only (85 °C, 16 h) 0.33%Pd-0.33%Au/TS-1 catalyst by X-ray energy dispersive spectroscopy (XEDS), revealed that the immobilized metal species existed as large Au-only nanoparticles, Au-rich alloys or sub-nano Pd-only clusters, notably no Pd-only nanoparticles were detected (Figures S.11-13). Upon exposure to calcination temperatures exceeding 200 °C it was possible to observe the agglomeration of metal species (Figure 5, with further data reported in Figures S.14-15), which aligns with our TEM (Table 1) and XPS (Figure S.8, Supplementary Note 3) analysis. A clear shift in nanoparticle composition was also observed, with the incorporation of Pd into the larger Au-rich nanoparticles (Figures S.14), the formation of Pd-only nanoparticles was also observed, which can be attributed to the agglomeration of the Pd clusters identified in the dried-only material. Such analysis, in addition

to our earlier studies, which revealed the limited activity of monometallic Au and Pd catalysts (Figure 2) and that of the dried-only 0.33%Pd-0.33%Au/TS-1 catalyst, (Figure 4) indicates that the presence of PdAu alloyed species is largely responsible for the observed reactivity towards cyclohexanone ammoximation. However, the minor contribution from elementally segregated species should not be disregarded.

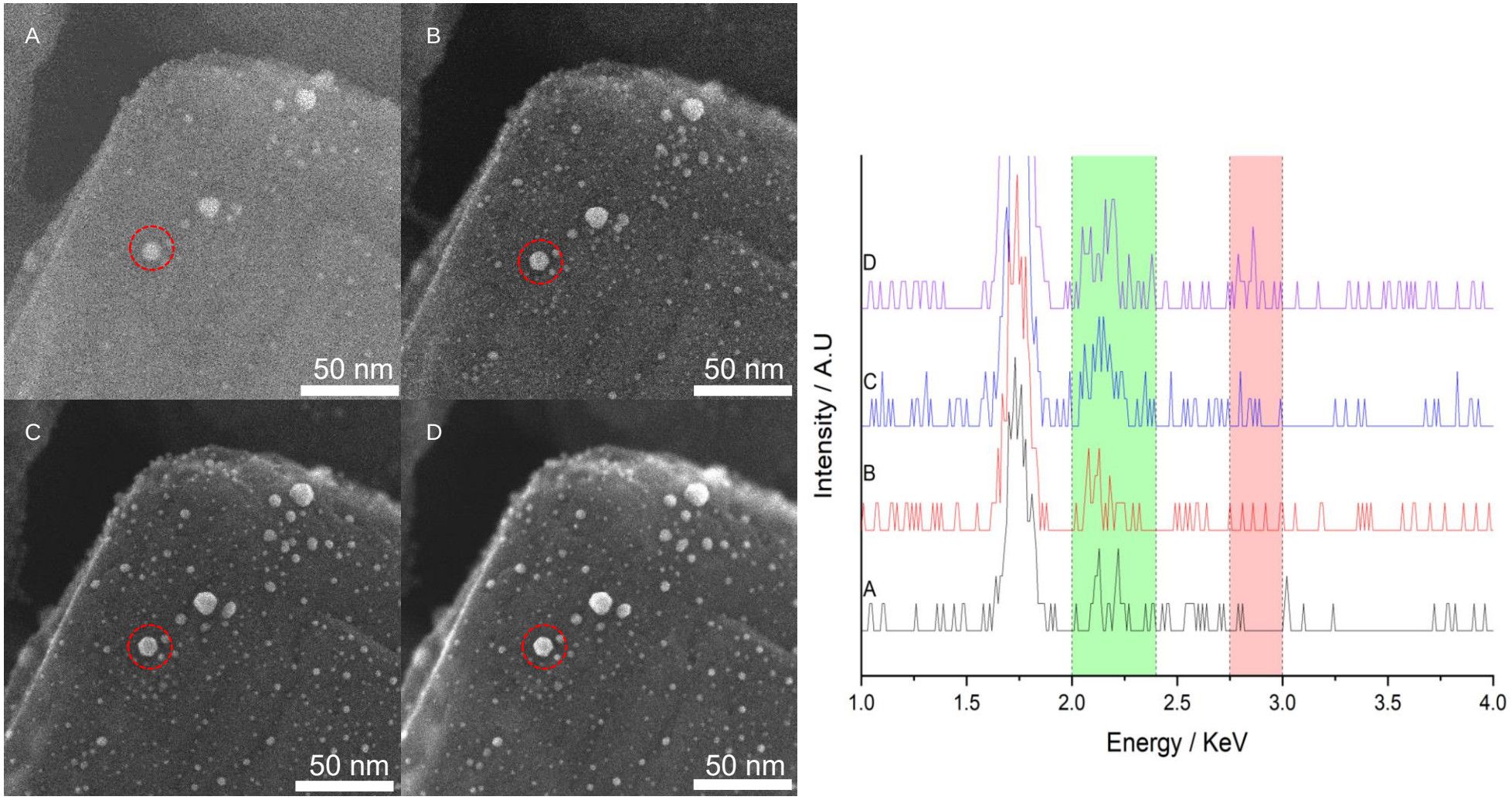

Figure 5. In-situ secondary electron (SE in STEM) imaging and corresponding XEDS analysis (Au (Mα) and Pd (Lα) centred at 2.12 and 2.84 KeV respectively) of the indicated nanoparticle demonstrating the formation of PdAu alloys as a result of exposure of the of the 0.33%Pd-0.33%Au/TS-1 catalyst to an oxidative thermal treatment. **(A)** Dried-only, **(B)** 200 °C, **(C)** 300 °C and **(D)** 400 °C. **Note:** The dried-only sample was exposed to 85 °C, static air, 16 h. **Conditions for calcination:** static air, 3 h, 10 °Cmin^{-1}.

Detailed analysis of the fresh 0.33%Pd-0.33%Au/TS-1 catalyst (calcined at 400 °C) by HAADF-STEM and XEDS elemental mapping (Figure 6, with additional data reported in Figures S.16-17) supported our in-situ analysis (Figure 5), and identified the presence of both Pd-only nanoparticles and PdAu nanoalloys. A bimodal particle size distribution and a distinctive relationship between particle size and elemental composition has been typically reported for PdAu catalysts prepared by the wet co-impregnation route to catalyst synthesis, where larger particles are found to be Au-rich, PdAu alloys, and the smaller nanoparticles consist of Pd-only (54,59). Similar observations can be made in this work, however, it is clear from our in-situ STEM analysis (Figure 5) that the PdAu nanoalloys exist over a large particle size range, whereas no large (> 20 nm) Pd-only species were observed.

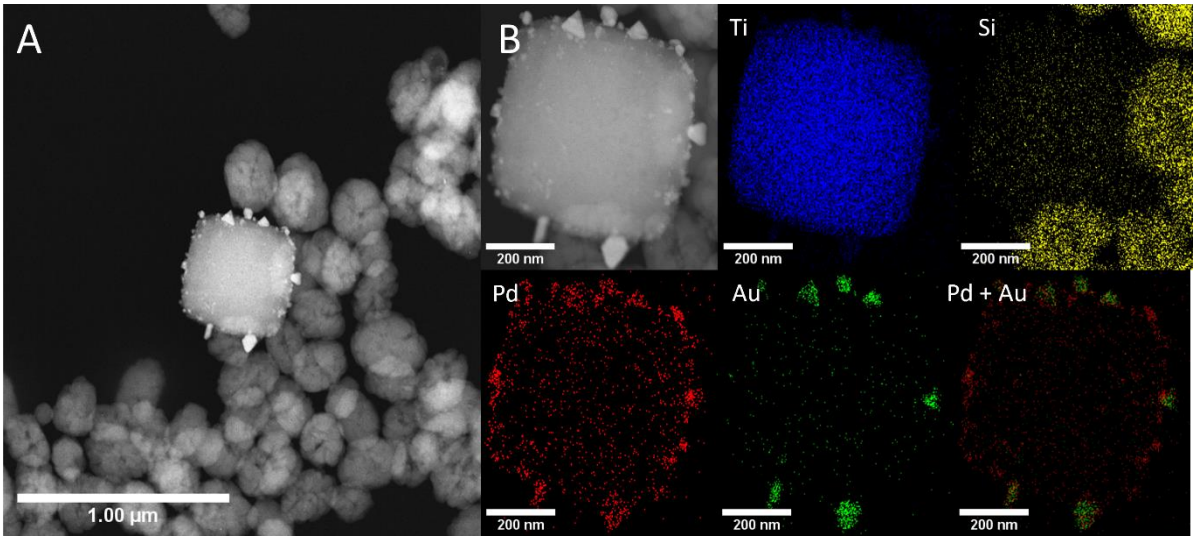

Figure 6. Microstructural analysis of the 0.33%Pd-0.33%Au/TS-1 catalyst including a **(A)** HAADF-STEM image showing the preferential deposition of precious metal nanoparticles onto the TiO_2 minority component and **(B)** HAADF-STEM image and XEDS mapping of highlighted area showing the presence of PdAu alloys and smaller Pd nanoparticles, Au (green), Pd (red),Ti (blue) and Si (yellow).

With the leaching of metal species during use in the in-situ ammoximation reaction established (Table S.9) and with a particular focus on the 0.33%Pd-0.33%Au/TS-1 catalyst exposed to a high-temperature oxidative heat treatment (400 °C); we next investigated catalyst stability upon reuse (Figure S.18) and determined that there was no loss in reactivity, despite the observed loss of Pd. Analysis of the used 0.33%Pd-0.33%Au/TS-1 catalyst by HAADF-STEM and XEDS correlates well with our ICP-MS analysis and identified that the Pd leaching is associated with the loss of the unalloyed Pd species, whereas the PdAu nanoparticles were retained after use (Figure S.19). We next conducted a series of hot-filtration experiments to identify the contribution of homogeneous metal species to the observed reactivity (Figure 7. A-B). In the absence of the heterogeneous catalyst, no additional cyclohexanone conversion was observed, with this metric identical to that during the initial 1.5 h reaction, which was

conducted in the presence of the 0.33%Pd-0.33%Au/TS-1 catalyst (20% cyclohexanone conversion). To determine if the inactivity observed during the two-part hot-filtration experiment was due to the removal of the TS-1 component, a further hot-filtration experiment was conducted whereby, after the initial 1.5 h experiment the heterogeneous catalyst was replaced with an equivalent amount of bare TS-1 (0.075 g), prior to replacing the reactant gases and re-commencing the reaction for a further 1.5 h. Some additional conversion of cyclohexanone was detected (24% cyclohexanone conversion at 3 h). While this may be indicative of a homogeneous component to the reaction it is notable that we did not observe any additional formation of cyclohexanone oxime. This in addition to the loss in selectivity to desired products in the second part of the hot-filtration experiment, and the known ability of TS-1 to catalyse unselective side reactions(60) indicates that the contribution of any leached metal species towards cyclohexanone ammoximation, if any, is negligible and that in the absence of the heterogenous metal loaded catalyst the TS-1 component alone is responsible for the observed increase in cyclohexanone conversion.

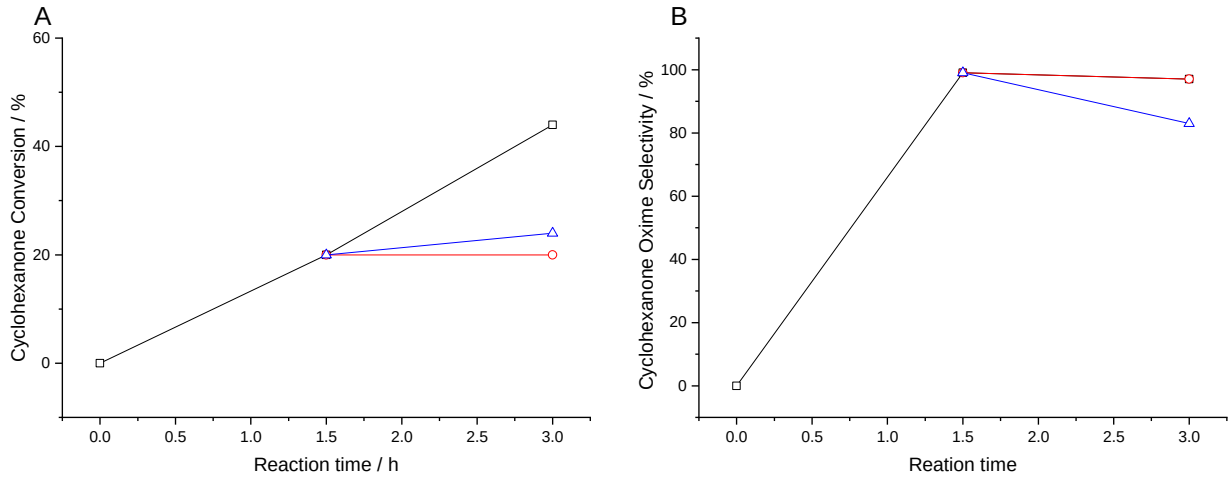

Figure 7. Efficacy of leached species in the ammoximation of cyclohexanone as identified by a hot filtration experiment using the 0.33%Pd-0.33%Au/TS-1 catalyst. **(A)** Cyclohexanone conversion and **(B)** cyclohexanone oxime selectivity. ***Key:*** Heterogeneous catalysed reaction (*black squares*); hot filtration reaction where the catalyst was removed by filtration prior to a final 1.5 h experiment (*red circles*); hot filtration where the catalyst was removed by filtration after 1.5 h and replaced by TS-1 for the final 1.5 h of reaction (*blue triangles*). **Note 1:** Catalyst exposed to an oxidative heat treatment (3 h, 400 °C, 10 °Cmin^{-1}, static air) prior to use. **Note 2:** In the case of the hot filtration experiment where the heterogeneous 0.33%Pd-0.33%Au/TS-1 catalyst was replaced with TS-1 (0.075 g), the TS-1 catalyst was used as received. **Ammoximation reaction conditions:** Cyclohexanone (2 mmol), NH_4HCO_3 (4 mmol), 5% H_2/N_2 (420 psi), 25% O_2/N_2 (160 psi), catalyst (0.075 g), t-BuOH (5.9 g), H_2O (7.5 g), reaction time 3 h, reaction temperature 80 ^{O}C, stirring speed 800 rpm.

Finally, again utilising the optimal 0.33%Pd-0.33%Au/TS-1 catalyst, we extended our studies to assess catalytic performance towards the ammoximation of a small range of other ketones (cyclopentanone, cycloheptanone, cyclooctanone and cyclododecanone) (Figure 8), with many of the corresponding oximes finding application in both the pharmaceutical and polymer industries.(61,62) Regardless of substrate, selectivity towards the corresponding oxime was found to be high (≥ 90% in all cases), demonstrating the versatility of the in-situ approach to oxime formation. However, the extent of substrate conversion was found to differ over the series of ketones investigated. This is in keeping with previous studies utilising commercial H_2O_2, with the variation in the rate of ketone conversion considered to be primarily related to the differing intrinsic reactivity of the ketones with hydroxylamine, in addition to the limited ability of the larger ketones to access the interior pore structure of the titanosilicate.(63)

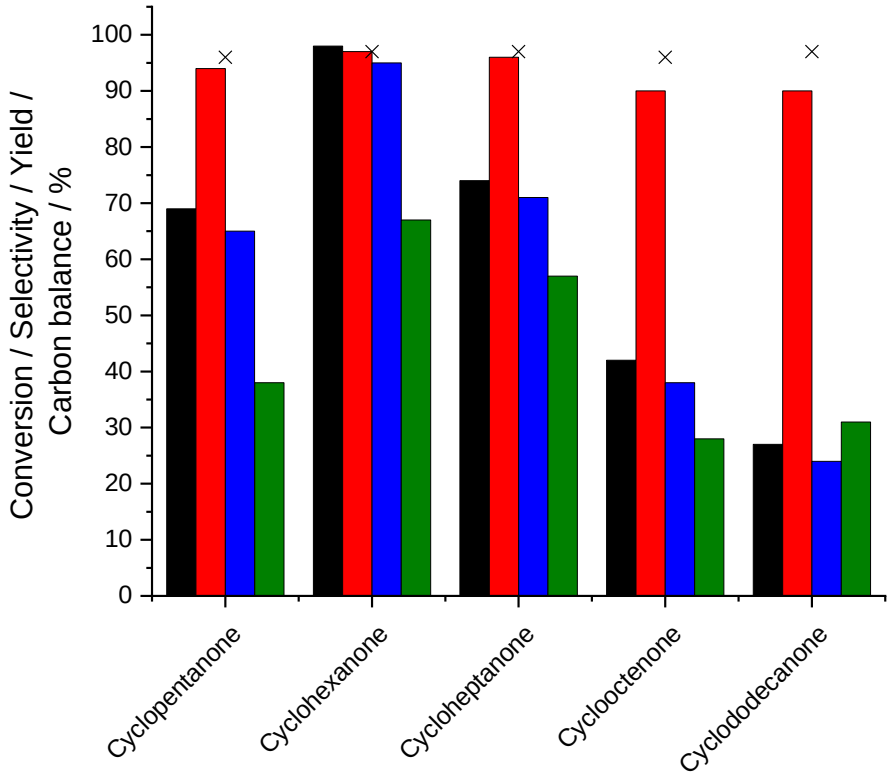

Figure 8. Catalytic activity of the 0.33%Au-0.33%Pd/TS-1 catalyst towards the ammoximation of a range of ketones, via the *in-situ* production of H_2O_2. ***Key*****;** Ketone conversion *(black bars*), oxime selectivity (*red bars*), oxime yield (*blue bars*), H_2 selectivity (*green bars*) and carbon balance (*crosses*). **Ammoximation reaction conditions:** Ketone (2 mmol), NH_4HCO_3 (4 mmol), 5%H_2/N_2 (420 psi), 25%O_2/N_2 (160 psi), catalyst (0.075 g), t-BuOH (5.9 g), H2O (7.5 g), 6 h, 80 °C, 800 rpm.

Conclusion and Future Perspectives.

The in-situ synthesis of H_2O_2 over a bi-functional composite catalyst that is able to both synthesise H_2O_2 and utilise it in the formation of the hydroxylamine intermediate represents an attractive alternative to the current industrial route to the ammoximation of cyclohexanone and other ketones to the corresponding oxime.

Within this work we have demonstrated that using Pd-based nanoalloys supported on a commercially available TS-1 it is indeed possible to bridge the wide conditions gap that exists between the individual reaction pathways (H_2O_2 synthesis and ketone ammoximation), and achieve selectivities and product yields approaching 100%. In particular, the alloying of Pd with Au was found to significantly improve catalytic activity. This is despite the higher H_2O_2 synthesis rates observed over the monometallic Pd catalyst and is attributed to the ability of Au to modify Pd speciation, inhibit competitive H_2O_2 degradation pathways (leading to enhanced H_2 utilisation) and promote the release of the oxidant from metal surfaces for utilisation by the TS-1 component. Notably, the formation of PdAu nanoalloys was also found to correlate with an improvement in catalyst stability.

It is considered that the in-situ approach developed herein for ketone ammoximation could form the basis of an alternative route to numerous chemical transformations that are currently dependent on a combination of preformed H_2O_2 and TS-1 while allowing for significant process intensification. However, with a particular focus on the ammoximation of cyclohexanone, it is suggested that future studies be focused on the iterative development of both catalytically active species, *i.e.* the Ti^{IV} centres within the TS-1 component and metal sites responsible for H_2O_2 production. There is still clearly a need for improvements in catalyst reactivity and selective H_2 utilisation to be made, while diffusion limitations associated with the TS-1 pore structure should also be considered.

Furthermore, the loss of TS-1 crystallinity and formation of TiO_2 surface species is well known to result from the presence of ammonia in reactant streams and lead to catalyst deactivation during industrial use as well as promoting precious metal dissolution. While significant improvements in TS-1 stability have been made in recent years there is a need to evaluate the long-term stability of immobilised metal species under real-world conditions and over extended time frames.

Graphical abstract.

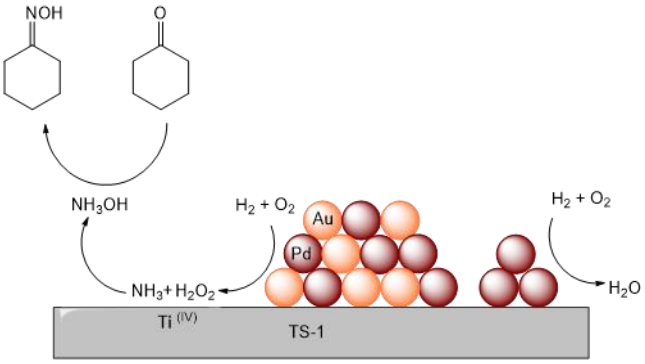

Supporting Information.

Data relating to catalytic activity towards the direct synthesis and subsequent degradation of H_2O_2 and the in-situ oxidation of cyclohexanone to the corresponding oxime, with accompanying characterisation of catalytic materials via XRD, FTIR, XPS, CO-DRIFTS, TEM, HAADF-STEM and X-EDS.

Acknowledgements.

We appreciate technical support from Mr Hiroaki Matsumoto and Mr Chaobin Zeng, Hitachi High-Technologies (Shanghai) Co. Ltd, for HR-STEM characterization. The authors would like to thank the CCI-Electron Microscopy Facility which has been part-funded by the European Regional Development Fund through the Welsh Government, and The Wolfson Foundation. XPS data collection was performed at the EPSRC National Facility for XPS (‘HarwellXPS’), operated by Cardiff University and UCL, under contract No. PR16195. **Funding:** The authors thank UBE Corporation for financial support R.J.L, A.S and G.J.H gratefully acknowledge Cardiff University and the Max Planck Centre for Fundamental Heterogeneous Catalysis (FUNCAT) for financial support. X.L. acknowledges financial support from National Key R&D Program of China (2021YFA1500300) and National Natural Science Foundation of China (21872163 and 22072090). S.J.F acknowledges the award of a Prize Research Fellowship from the University of Bath.

Author Contributions.

R.J.L, K.U, Y.F, S.J.F and G.J.H contributed to the design of the study; R.J.L and K.U conducted experiments and data analysis. R.J.L, K.U, X.L, Y.F, J.S, J.K.E, S.J.F, C.J.K, L.C,

Y.Y and G.J.H provided technical advice and result interpretation. R.J.L, X.L, T.Q, T.E.D, D.J.M, A.S and C.J.K conducted catalyst characterization and corresponding data processing. R.J.L, wrote the manuscript and the supplementary material, all authors commented on and amended both documents. All authors discussed and contributed to the work.

Competing Interests.

The authors declare no competing interests.

References.

1. Taramasso, M.; Perego, G.; Notari, B.; (Montedipe SpA), US 4410501A, 1983.
2. Puértolas, B.; Hill, A. K.; García, T.; Solsona, B.; Torrente-Murciano, L., In-situ synthesis of hydrogen peroxide in tandem with selective oxidation reactions: A mini-review. *Catal. Today,* **2015**, 248, 115-127, DOI: 10.1016/j.cattod.2014.03.054.
3. Luo, Y.; Xiong, J.; Pang, C.; Li, G.; Hu, C., Direct Hydroxylation of Benzene to Phenol over TS-1 Catalysts. *Catalysts,* **2018**, 8 (2), 49. DOI: 10.3390/catal8020049
4. Schuster, W.; Niederer, J. P. M.; Hoelderich, W. F., The gas phase oxidative dehydrogenation of propane over TS-1. DOI: 10.1016/S0926-860X(00)00749-3 *Appl. Catal., A.* **2001**, 209 (1), 131-143.
5. Aly, M.; Saeys, M., Selective silylation boosts propylene epoxidation with H_2 and O_2 over Au/TS-1. *Chem Catalysis,* **2021**, 1 (4), 761-762. DOI: 10.1016/j.checat.2021.07.004
6. Lin, M.; Xia, C.; Zhu, B.; Li, H.; Shu, X., Green and efficient epoxidation of propylene with hydrogen peroxide (HPPO process) catalyzed by hollow TS-1 zeolite: A 1.0 kt/a pilot-scale study. *Chem. Eng. J.* **2016**, 295, 370. DOI: 10.1016/j.cej.2016.02.072
7. Wang, G.; Du, W.; Duan, X.; Cao, Y.; Zhang, Z.; Xu, J.; Chen, W.; Qian, G.; Yuan, W.; Zhou, X.; Chen, D., Mechanism-guided elaboration of ternary Au–Ti–Si sites to boost propylene oxide formation. *Chem Catalysis* **2021**, 1 (4), 885-895. DOI: 10.1016/j.checat.2021.06.006
8. Liu, G.; Wu, J.; Luo, H., Ammoximation of Cyclohexanone to Cyclohexanone Oxime Catalyzed by Titanium Silicalite-1 Zeolite in Three-phase System. *Chin. J. Chem. Eng.* **2012,** 20, 889. DOI: 10.1016/S1004-9541(12)60414-5
9. HDIN Research, Global Nylon 6 Production Capacity reach to 8.86 million Tons in 2024 (2019) via https://www.hdinresearch.com/news/56, accessed on 21.7.22.
11. Mokaya, R.; Poliakoff, M., A Cleaner Way to Nylon? *Nature* **2005,** 437 (7063), 1243-1244. DOI: 10.1038/4371243a
12. Mantegazza, M. A.; Cesana, A.; Pastori, M., Ammoximation of ketones on titanium silicalite. A study of the reaction byproducts. *Top. Catal.,* **1996,** 3 (3), 327-335. DOI: 10.1007/BF02113858

13. Yip, A. C. K.; Hu, X., Catalytic Activity of Clay-Based Titanium Silicalite-1 Composite in Cyclohexanone Ammoximation. *Ind. Eng. Chem. Res.,* **2009,** 48 (18), 8441-8450. DOI: 10.1021/ie900731s.
14. Qi, Y.; Ye, C.; Zhuang, Z.; Xin, F., Preparation and evaluation of titanium silicalite-1 utilizing pretreated titanium dioxide as a titanium source. *Microporous Mesoporous Mater.,* **2011,** 142 (2), 661-665. DOI: 10.1016/j.micromeso.2011.01.012
15. Dal Pozzo, L.; Fornasari, G.; Monti, T., TS-1, catalytic mechanism in cyclohexanone oxime production *Catal. Commun.,* **2002,** 3, 369. DOI: 10.1016/S1566-7367(02)00145-0
16. Yip, A. C. K.; Hu, X., Formulation of Reaction Kinetics for Cyclohexanone Ammoximation Catalyzed by a Clay-Based Titanium Silicalite-1 Composite in a Semibatch Process *Ind. Eng. Chem. Res.,* **2011,** 50 (24), 13703-13710. DOI: 10.1021/ie201467u.
17. Lewis, R. J.; Hutchings, G. J., Recent Advances in the Direct Synthesis of H_2O_2 *ChemCatChem,* **2019,** 11, 298. DOI: 10.1002/cctc.201801435
18. Edwards, J. K.; Freakley, S. J.; Lewis, R. J.; Pritchard, J. C.; Hutchings, G. J., Advances in the direct synthesis of hydrogen peroxide from hydrogen and oxygen. *Catal. Today,* **2015,** 248, 3-9. DOI: 10.1016/j.cattod.2014.03.011
19. Campos-Martin, J. M.; Blanco-Brieva, G.; Fierro, J. L. G., Hydrogen Peroxide Synthesis: An Outlook beyond the Anthraquinone Process. *Angew. Chem. Int. Ed.,* **2006,** 45 (42), 6962-6984.DOI: 10.1002/anie.200503779.
20. Gao, G.; Tian, Y.; Gong, X.; Pan, Z.; Yang, K.; Zong, B., Advances in the production technology of hydrogen peroxide *Chin. J. Catal.,* **2020,** 41 (7), 1039-1047. DOI: 10.1016/S1872-2067(20)63562-8
21. Liang, X.; Mi, Z.; Wang, Y.; Wang, L.; Zhang, X., Synthesis of acetone oxime through acetone ammoximation over TS-1. *React. Kinet. Catal. Lett.,* **2004,** 82 (2), 333-337. DOI: 10.1023/B:REAC.0000034845.65961.3e
22. Zajacek, J. G.; Crocco, G. L.; Jubin, J. C (Lyondell Chemical Technology LP) EP 0690045A1, 1994
23. Lewis, R. J.; Ueura, K.; Liu, X.; Fukuta, Y.; Davies, T. E.; Morgan, D. J.; Chen, L.; Qi, J.; Singleton, J.; Edwards, J. K.; Freakley, S. J.; Kiely, C. J.; Yamamoto, Y.; Hutchings, G. J., Highly efficient catalytic production of oximes from ketones using in situ–generated H_2O_2. *Science,* **2022,** 376 (6593), 615-620. DOI: 10.1126/science.abl4822
24. Gallina, G.; García-Serna, J.; Salmi, T. O.; Canu, P.; Biasi, P., Bromide and Acids: A Comprehensive Study on Their Role on the Hydrogen Peroxide Direct Synthesis. *Ind. Eng. Chem. Res.* **2017,** 56, 13367. DOI: 10.1021/acs.iecr.7b01989
25. Liu, Q.; Gath, K. K.; Bauer, J. C.; Schaak, R. E.; Lunsford, J. H., The Active Phase in the Direct Synthesis of H_2O_2 from H_2 and O_2 over Pd/SiO_2 Catalyst in a H_2SO_4 /Ethanol System. *Catal. Lett.* **2009,** 132, 342. DOI: 10.1007/s10562-009-0104-y

26. Liu, Q.; Bauer, J. C.; Schaak, R. E.; Lunsford, J. H., Direct synthesis of H_2O_2 from H_2 and O_2 over Pd–Pt/SiO_2 bimetallic catalysts in a H_2SO_4/ethanol system. *Appl. Catal., A* **2008,** 339, 130. DOI: 10.1016/j.apcata.2008.01.026
27. Santos, A.; Lewis, R. J.; Malta, G.; Howe, A. G. R.; Morgan, D. J.; Hampton, E.; Gaskin, P.; Hutchings, G. J., Direct Synthesis of Hydrogen Peroxide over Au–Pd Supported Nanoparticles under Ambient Conditions. *Ind. Eng. Chem. Res.,* **2019,** 58 (28), 12623-12631. DOI: 10.1021/acs.iecr.9b02211
28. Lewis, R. J.; Ueura, K.; Fukuta, Y.; Freakley, S. J.; Kang, L.; Wang, R.; He, Q.; Edwards, J. K.; Morgan, D. J.; Yamamoto, Y.; Hutchings, G. J., The Direct Synthesis of H_2O_2 Using TS-1 Supported Catalysts *ChemCatChem,* **2019,** 11, 1673. DOI: 10.1002/cctc.201900100.
29. Wu, C.; Wang, Y.; Mi, Z.; Xue, L.; Wu, W.; Min, E.; Han, S.; He, F.; Fu, S., Effects of organic solvents on the structure stability of TS-1 for the ammoximation of cyclohexanone. *React. Kinet. Catal. Lett.,* **2002,** 77 (1), 73-81. DOI: 10.1023/A:1020391803295.
30. Wilson, N. M.; Priyadarshini, P.; Kunz, S.; Flaherty, D. W., Direct synthesis of H_2O_2 on Pd and Au_xPd_1 clusters: Understanding the effects of alloying Pd with Au. *J. Catal.* **2018,** 357, 163.DOI: 10.1016/j.jcat.2017.10.028.
31. Ntainjua N, E.; Edwards, J. K.; Carley, A. F.; Lopez-Sanchez, J. A.; Moulijn, J. A.; Herzing, A. A.; Kiely, C. J.; Hutchings, G. J., The role of the support in achieving high selectivity in the direct formation of hydrogen peroxide. *Green Chem.,* **2008,** 10 (11), 1162-1169. DOI: 10.1039/B809881F.
32. Menegazzo, F.; Manzoli, M.; Signoretto, M.; Pinna, F.; Strukul, G., H_2O_2 direct synthesis under mild conditions on Pd–Au samples: Effect of the morphology and of the composition of the metallic phase. *Catal. Today,* **2015,** 248, 18-27. DOI: 10.1016/j.cattod.2014.01.015.
33. Brehm, J.; Lewis, R. J.; Morgan, D. J.; Davies, T. E.; Hutchings, G. J., The Direct Synthesis of Hydrogen Peroxide over AuPd Nanoparticles: An Investigation into Metal Loading. *Catal. Lett.,* **2022,** 152 (1), 254-262. DOI: 10.1007/s10562-021-03632-6.
34. Kanungo, S.; van Haandel, L.; Hensen, E. J. M.; Schouten, J. C.; Neira d'Angelo, M. F., Direct synthesis of H_2O_2 in AuPd coated micro channels: An in-situ X-Ray absorption spectroscopic study. *J. Catal.* **2019,** 370, 200. DOI: 10.1016/j.jcat.2018.12.017.
35. Edwards, J. K.; Hutchings, G. J., Palladium and Gold–Palladium Catalysts for the Direct Synthesis of Hydrogen Peroxide. *Angew. Chem., Int. Ed.* **2008,** 47, 9192.DOI: 10.1002/anie.200802818.
36. Lewis, R. J.; Ueura, K.; Fukuta, Y.; Davies, T. E.; Morgan, D. J.; Paris, C. B.; Singleton, J.; Edwards, J. K.; Freakley, S. J.; Yamamoto, Y.; Hutchings, G. J., Cyclohexanone

ammoximation via in situ H_2O_2 production using TS-1 supported catalysts. *Green Chem.,* **2022**. DOI: 10.1039/d2gc02689a.

37. Zhao, S.; Xie, W.; Yang, J.; Liu, Y.; Zhang, Y.; Xu, B.; Jiang, J.; He, M.; Wu, P., An investigation into cyclohexanone ammoximation over Ti-MWW in a continuous slurry reactor. *Appl. Catal., A.,* **2011,** 394 (1), 1-8. DOI: 10.1016/j.apcata.2010.10.037.
38. Li, Z.; Gao, L.; Zhu, X.; Ma, W.; Feng, X.; Zhong, Q., Synergistic Enhancement over Au-Pd/TS-1 Bimetallic Catalysts for Propylene Epoxidation with H_2 and O_2. *ChemCatChem,* **2019,** 11 (20), 5116-5123.DOI: 10.1002/cctc.201900845.
39. Edwards, J. K.; Solsona, B.; N, E. N.; Carley, A. F.; Herzing, A. A.; Kiely, C. J.; Hutchings, G. J., Switching Off Hydrogen Peroxide Hydrogenation in the Direct Synthesis Process. *Science,* **2009,** 323, 1037. DOI: 10.1126/science.1168980
40. Agarwal, N.; Thomas, L.; Nasrallah, A.; Sainna, M. A.; Freakley, S. J.; Edwards, J. K.; Catlow, C. R. A.; Hutchings, G. J.; Taylor, S. H.; Willock, D. J., The direct synthesis of hydrogen peroxide over Au and Pd nanoparticles: A DFT study. *Catal. Today,* **2021,** 381, 76-85. DOI: 10.1016/j.cattod.2020.09.001.
41. Kesavan, L.; Tiruvalam, R.; Rahim, M. H. A.; bin Saiman, M. I.; Enache, D. I.; Jenkins, R. L.; Dimitratos, N.; Lopez-Sanchez, J. A.; Taylor, S. H.; Knight, D. W.; Kiely, C. J.; Hutchings, G. J., Solvent-free oxidation of primary carbon-hydrogen bonds in toluene using Au-Pd alloy nanoparticles. *Science,* **2011,** 331 (6014), 195-199. DOI: 10.1126/science.1198458.
42. Chang, C.; Long, B.; Yang, X.; Li, J., Theoretical Studies on the Synergetic Effects of Au–Pd Bimetallic Catalysts in the Selective Oxidation of Methanol. J. Phys. Chem. C., **2015,** 119 (28), 16072-16081. DOI: 10.1021/acs.jpcc.5b03965
43. Crombie, C. M.; Lewis, R. J.; Taylor, R. L.; Morgan, D. J.; Davies, T. E.; Folli, A.; Murphy, D. M.; Edwards, J. K.; Qi, J.; Jiang, H.; Kiely, C. J.; Liu, X.; Skjøth-Rasmussen, M. S.; Hutchings, G. J., Enhanced Selective Oxidation of Benzyl Alcohol via In Situ H_2O_2 Production over Supported Pd-Based Catalysts. *ACS Catal.,* **2021,** 11 (5), 2701-2714. DOI: 10.1021/acscatal.0c04586.
44. Xu, G.; Yu, A.; Xu, Y.; Sun, C., Selective oxidation of methane to methanol using AuPd@ZIF-8. *Catal. Commun.* **2021,** 158, 106338. DOI : 10.1016/j.catcom.2021.106338
45. Chen, M.; Kumar, D.; Yi, C. W.; Goodman, D. W., The Promotional Effect of Gold in Catalysis by Palladium-Gold *Science* **2005,** 310 (5746), 291. DOI: DOI: 10.1126/science.1115800.
46. Gong, X.; Lewis, R. J.; Zhou, S.; Morgan, D. J.; Davies, T. E.; Liu, X.; Kiely, C. J.; Zong, B.; Hutchings, G. J., Enhanced catalyst selectivity in the direct synthesis of H_2O_2 through Pt incorporation into TiO2 supported AuPd catalysts. *Catal. Sci. Technol.,* **2020,** 10, 4635. DOI: doi.org/10.1039/D0CY01079K

47. Ricciardulli, T.; Gorthy, S.; Adams, J. S.; Thompson, C.; Karim, A. M.; Neurock, M.; Flaherty, D. W., Effect of Pd Coordination and Isolation on the Catalytic Reduction of O_2 to H_2O_2 over PdAu Bimetallic Nanoparticles. *J. Am. Chem. Soc.,* **2021,** 143 (14), 5445-5464. DOI: 10.1021/jacs.1c00539

48. Yao, Z.; Zhao, J.; Bunting, R. J.; Zhao, C.; Hu, P.; Wang, J., Quantitative Insights into the Reaction Mechanism for the Direct Synthesis of H_2O_2 over Transition Metals: Coverage-Dependent Microkinetic Modeling. *ACS Catal.,* **2021,** 11 (3), 1202-1221. DOI: 10.1021/acscatal.0c04125.

49. Edwards, J. K.; Parker, S. F.; Pritchard, J.; Piccinini, M.; Freakley, S. J.; He, Q.; Carley, A. F.; Kiely, C. J.; Hutchings, G. J., Effect of acid pre-treatment on AuPd/SiO_2 catalysts for the direct synthesis of hydrogen peroxide/ *Catal. Sci. Technol.,* **2013,** 3 (3), 812-818. DOI: 10.1039/C2CY20767B.

50. Ouyang, L.; Tian, P.; Da, G.; Xu, X.; Ao, C.; Chen, T.; Si, R.; Xu, J.; Han, Y., The origin of active sites for direct synthesis of H_2O_2 on Pd/TiO_2 catalysts: Interfaces of Pd and PdO domains. *J. Catal.* **2015,** 321, 70. DOI: 10.1016/j.jcat.2014.10.003.

51. Wilson, A. R.; Sun, K.; Chi, M.; White, R. M.; LeBeau, J. M.; Lamb, H. H.; Wiley, B. J., From Core–Shell to Alloys: The Preparation and Characterization of Solution-Synthesized AuPd Nanoparticle Catalysts. *J. Phys. Chem. C,* **2013,** 117 (34), 17557-17566. DOI: 10.1021/jp404157m.

52. Han, Y.; Zhong, Z.; Ramesh, K.; Chen, F.; Chen, L.; White, T.; Tay, Q.; Yaakub, S. N.; Wang, Z., Au Promotional Effects on the Synthesis of H_2O_2 Directly from H_2 and O_2 on Supported Pd−Au Alloy Catalysts. *J. Phys. Chem. C,* **2007,** 111 (24), 8410-8413. DOI: 10.1021/jp072934g

53. Drago, R. S.; Dias, S. C.; McGilvray, J. M.; Mateus, A. L. M. L., Acidity and Hydrophobicity of TS-1. *J. Phys. Chem. B.,* **1998,** 102 (9), 1508-1514. DOI: 10.1021/jp973249k

54. Herzing, A. A.; Watanabe, M.; Edwards, J. K.; Conte, M.; Tang, Z. R.; Hutchings, G. J.; Kiely, C. J., Energy dispersive X-ray spectroscopy of bimetallic nanoparticles in an aberration corrected scanning transmission electron microscope. *Faraday Discuss.* **2008,** 138, 337. DOI: doi.org/10.1039/B706293C

55. Sasirekha, N.; Sangeetha, P.; Chen, Y.-W., Bimetallic Au–Ag/CeO_2 Catalysts for Preferential Oxidation of CO in Hydrogen-Rich Stream: Effect of Calcination Temperature. *J. Phys. Chem. C,* **2014,** 118 (28), 15226-15233. DOI: 10.1021/jp500102g

56. Edwards, J. K.; Solsona, B. E.; Landon, P.; Carley, A. F.; Herzing, A.; Kiely, C. J.; Hutchings, G. J., Direct synthesis of hydrogen peroxide from H_2 and O_2 using TiO_2-supported Au–Pd catalysts. *J. Catal.* **2005,** 236, 69. DOI: 10.1016/j.jcat.2005.09.015

57. Cattaneo, S.; Freakley, S. J.; Morgan, D. J.; Sankar, M.; Dimitratos, N.; Hutchings, G. J., Cinnamaldehyde hydrogenation using Au–Pd catalysts prepared by sol

immobilisation. *Catal. Sci. Technol.,* **2018,** 8 (6), 1677-1685. DOI: 10.1039/C7CY02556D.

58. Crombie, C. M.; Lewis, R. J.; Kovačič, D.; Morgan, D. J.; Davies, T. E.; Edwards, J. K.; Skjøth-Rasmussen, M. S.; Hutchings, G. J., The Influence of Reaction Conditions on the Oxidation of Cyclohexane via the In-Situ Production of H_2O_2. *Catal. Lett.,* **2021,** 151 (1), 164-171.DOI: 10.1007/s10562-020-03281-1.
59. Edwards, J. K.; Carley, A. F.; Herzing, A. A.; Kiely, C. J.; Hutchings, G. J., Direct synthesis of hydrogen peroxide from H_2 and O_2 using supported Au–Pd catalysts. *Faraday Discuss.* **2008,** 138, 225. DOI: 10.1039/B705915A
60. Cesana, A.; Mantegazza, M. A.; Pastori, M., A study of the organic by-products in the cyclohexanone ammoximation. *J. Mol. Catal. A: Chem.,* **1997,** 117 (1), 367-373. DOI: 10.1016/S1381-1169(96)00296-8
61. Li, L.; Chen, M.; Jiang, F.-C., Design, synthesis, and evaluation of 2-piperidone derivatives for the inhibition of β-amyloid aggregation and inflammation mediated neurotoxicity *Bioorg. Med. Chem.* **2016,** 24 (8), 1853-1865. DOI: 10.1016/j.bmc.2016.03.010
62. Eickelberg, W.; Hoelderich, W. F., Beckmann-rearrangement of cyclododecanone oxime to ω-laurolactam in the gas phase *J. Catal.,* **2009,** 263 (1), 42-55. DOI: 10.1016/j.jcat.2009.01.010
63. Wu, P.; Komatsu, T.; Yashima, T., Ammoximation of Ketones over Titanium Mordenite *J. Catal.,* **1997,** 168 (2), 400-411. DOI: 10.1006/jcat.1997.1679